The structural and depositional context and a new age estimate of the type Sierra Ladrones Formation in the southern Albuquerque Basin and vicinity, central New Mexico

David W. Love, David J. McCraw, Richard M. Chamberlin, Matthew Heizler, and Alex Rinehart
2022, pp. 239-251. https://doi.org/10.56577/FFC-72.239
Supplemental data: https://nmgs.nmt.edu/repository/index.cfml?rid=2022003

in:

Socorro Region III, Koning, Daniel J.; Hobbs, Kevin J.; Phillips, Fred M.; Nelson, W. John; Cather, Steven M.; Jakle, Anne C.; Van Der Werff, Brittney, New Mexico Geological Society 72nd Annual Fall Field Conference Guidebook, 426 p. https://doi.org/10.56577/FFC-72

This page is intentionally left blank to maintain order of facing pages.

New Mexico Geological Society Guidebook, 72nd Fall Field Conference, 2022, p. 239–251.

THE STRUCTURAL AND DEPOSITIONAL CONTEXT AND A NEW AGE ESTIMATE OF THE TYPE SIERRA LADRONES FORMATION IN THE SOUTHERN ALBUQUERQUE BASIN AND VICINITY, CENTRAL NEW MEXICO

DAVID W. LOVE[1], DAVID J. MCCRAW[1], RICHARD M. CHAMBERLIN[1], MATTHEW HEIZLER[1], AND ALEX RINEHART[2]

[1]New Mexico Bureau of Geology and Mineral Resources, New Mexico Institute of Mining and Technology, 801 Leroy Place, Socorro, NM 87801; david.love@nmt.edu

[2]Earth and Environmental Science Department, New Mexico Institute of Mining and Technology, 801 Leroy Place, Socorro, NM 87801

Abstract—The type Sierra Ladrones Formation is exposed between two north-trending, Quaternary normal faults and crossed by the east-flowing Rio Salado, on the southwest side of the Albuquerque Basin and the northwestern side of the Socorro Basin of the Rio Grande rift in central New Mexico. This article summarizes recent work on the two sedimentary facies of the type Sierra Ladrones Formation—fluvial facies of the ancestral Rio Grande and the piedmont alluvial facies interfingering with and overlying it. We obtained a $^{40}Ar/^{39}Ar$ age spectrum for detrital sanidines, indicating a maximum depositional age of 5.36 Ma in the lowest exposures of fluvial facies near the type area. Outcrops of the Sierra Ladrones Formation fluvial facies are bracketed by the Loma Pelada (west) and Loma Blanca (east) faults; these continue across the boundary between the southwestern Albuquerque Basin and northern Socorro Basin. The fluvial facies was transported to the south into the Socorro Basin, whereas the piedmont alluvial facies was transported north-northeast between the faults and on the Loma Blanca hanging wall. The apparent source of most of the piedmont alluvial facies south of the Rio Salado is the uplift of the Lemitar Mountains, its northern extension, and the Cerritos de las Minas. North of the Rio Salado, the piedmont alluvium has contributions from other sources, the Ladron Mountains and an ancestral Rio Salado. Uplift of Loma Blanca on the boundary between the two structural basins apparently has eroded all the overlying piedmont deposits seen to the north and south, whereas a >85 m thick section of piedmont deposits is preserved on the hanging wall of the Loma Blanca fault, with a vertical offset of at least 155 m. The piedmont alluvium on the hanging wall of the Loma Blanca fault within a kilometer of the fault contains no debris from the fluvial facies of the footwall. Two to three km east in the hanging wall, and down-section in piedmont and basin floor facies, pebble conglomerates exhibit paleo-transport ranging from northeast to southwest, suggesting a distributary system spread from a source to the northwest and north. Apparently the system was not influenced by a possibly uplifting basin divide to the south.

Although basin-fill outcrops on both sides of the Cliff fault in the southern Albuquerque Basin were included in the alluvial piedmont facies of the Sierra Ladrones Formation, recent work demonstrates that these deposits were deposited by the ancestral Rio Puerco (Ceja Formation) and Rio Salado drainages. The two drainages flowed southeast to join the ancestral Rio Grande, and perhaps their distal distributary system pushed the course of the Rio Grande eastward against the Joyita Hills uplift by ca. 3 Ma. The Ceja Formation crops out on the west side of the Rio Puerco Valley along the sides of Cañada Colorado and east-flowing drainages to the south. The Rio Puerco could only have advanced into this area after the axial river had abandoned the type Sierra Ladrones area. Piedmont alluvium similar to the Sierra Ladrones alluvial facies overlies these Rio Puerco pebbly sands of the Ceja Formation on both sides of the Loma Blanca fault, and both were transported to the southeast.

INTRODUCTION

The southern Albuquerque Basin of the Rio Grande rift in central New Mexico exhibits several structural, sedimentologic, and geomorphic oddities that extend into adjacent rift basins and motivate further studies. Most of the present features of the basins have developed over the past 5 million years (Hawley, 1978, 2005). After studying the evidence for long-term changes in courses of the Rio Grande, Rio Puerco, and several drainages from the east side of the basin over several decades (e.g., Love and Young, 1983; Lozinsky et al., 1991; Davis et al., 1993; Connell et al., 2005, 2013; Love and Rinehart, 2016), we explore the age of the arrival of the Rio Grande across the southern Albuquerque Basin and its course(s) south into the Socorro Basin. The sediments recording the arrival of the ancestral Rio Grande were named the Sierra Ladrones Formation by Machette (1978). The formation is a stack of fluvial and piedmont deposits exposed on the west side of the Albuquerque and northern Socorro Basins of the Rio Grande rift (Fig. 1 inset; Fig. 2). Although Machette did not measure or describe a type section, he indicated where the type area would be: the Sierra Ladrones label along a set of ridges east of the Ladron Mountains on a 1:250,000-scale Socorro topographic map. Machette (1978) mapped these axial and piedmont alluvial deposits as part of the Sierra Ladrones Formation on his geologic map of the San Acacia 7.5-minute quadrangle. He interpreted the age of the Sierra Ladrones Formation as early to late Pliocene. Connell and Lucas (2001) measured a 370 m section of the Sierra Ladrones Formation in the type area (Fig. 3, shown in Fig. 2). The base is not exposed, but Machette thought that a piedmont alluvial unit farther south underlaid the axial river facies. The upper strata of the measured section, and adjacent mapping by Connell and McCraw (2007), show interfingering of piedmont and axial facies with increased abundance of

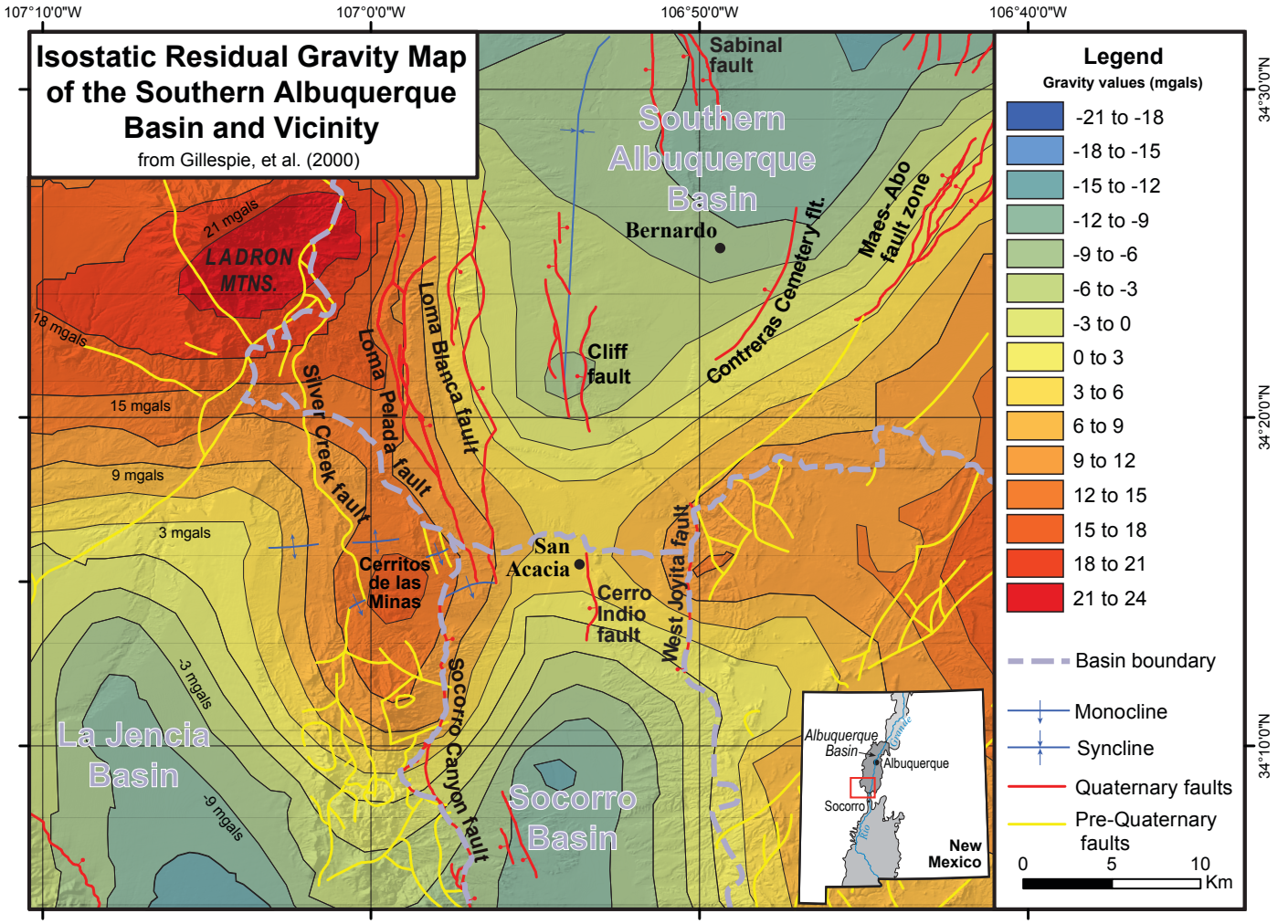

FIGURE 1. Contoured isostatic residual gravity map, modified from Gillespie et al. (2000) by Celep (2017) and this work, showing the boundaries between the southern Albuquerque Basin, the La Jencia Basin, and the Socorro Basin of the Rio Grande rift in central New Mexico. See Appendix 1 for detailed discussion of why the basin boundaries are drawn where they are. Faults with Quaternary movements in red; older faults in yellow; arches, synclines, and ramps are in blue.

piedmont alluvium toward the top of exposures (Fig. 3). Connell and McCraw (2007) showed that whereas the ancestral river deposits exhibited southward flow, many of the interfingering alluvial deposits flowed north or northeast. Chamberlin et al. (2001) mapped similar exposures of interfingering axial-fluvial and piedmont strata near the mouth San Lorenzo Canyon, 15 km to the south, with piedmont alluvium transported to the east and northeast. North of San Lorenzo Canyon, Machette (1978) mapped the distinct hill called Loma Blanca as composed exclusively of axial-fluvial facies. On the east side of Loma Blanca, Machette (1978) mapped a piedmont unit that he thought was older and underlaid the fluvial facies. We initially focused on this piedmont unit to look for a transition from piedmont alluvium to basal beds of the ancestral Rio Grande. Instead, Hinojosa (2021) and research by us show that this piedmont alluvium is younger and has been faulted downwards by the Loma Blanca fault alongside older exposures of the axial facies to the west. The piedmont alluvium next to the fault shows north-to-northeast transport and is not derived from the axial facies of the footwall of the fault.

In this article we synthesize this prior work and recent observations to place the fluvial and piedmont facies in a regional context and to develop an explanation as to why the piedmont facies in the immediate Loma Blanca fault hanging wall, south of the Rio Salado, exhibit NNE paleoflow indicators. The overarching impetus of this study is documenting changing paleo-depositional environments in the Pliocene, starting with the ancestral Rio Grande having crossed the inter-basin divide north-south on the west side of the basins, and presenting data documenting that the piedmont alluvial unit crossed the same area transporting sediments in the opposite direction. This paper also presents a new maximum depositional age estimate for the fluvial sand, leading to implications for the age of the overlying piedmont alluvium.

PREVIOUS WORK

The Sierra Ladrones fluvial deposits have been mapped from north to south across the La Joya NW (Connell and McCraw, 2007), San Acacia (Machette, 1978), and Lemitar (Chamberlin et al., 2001) 7.5-minute quadrangles, which cover the majority of our study area (mapped latest

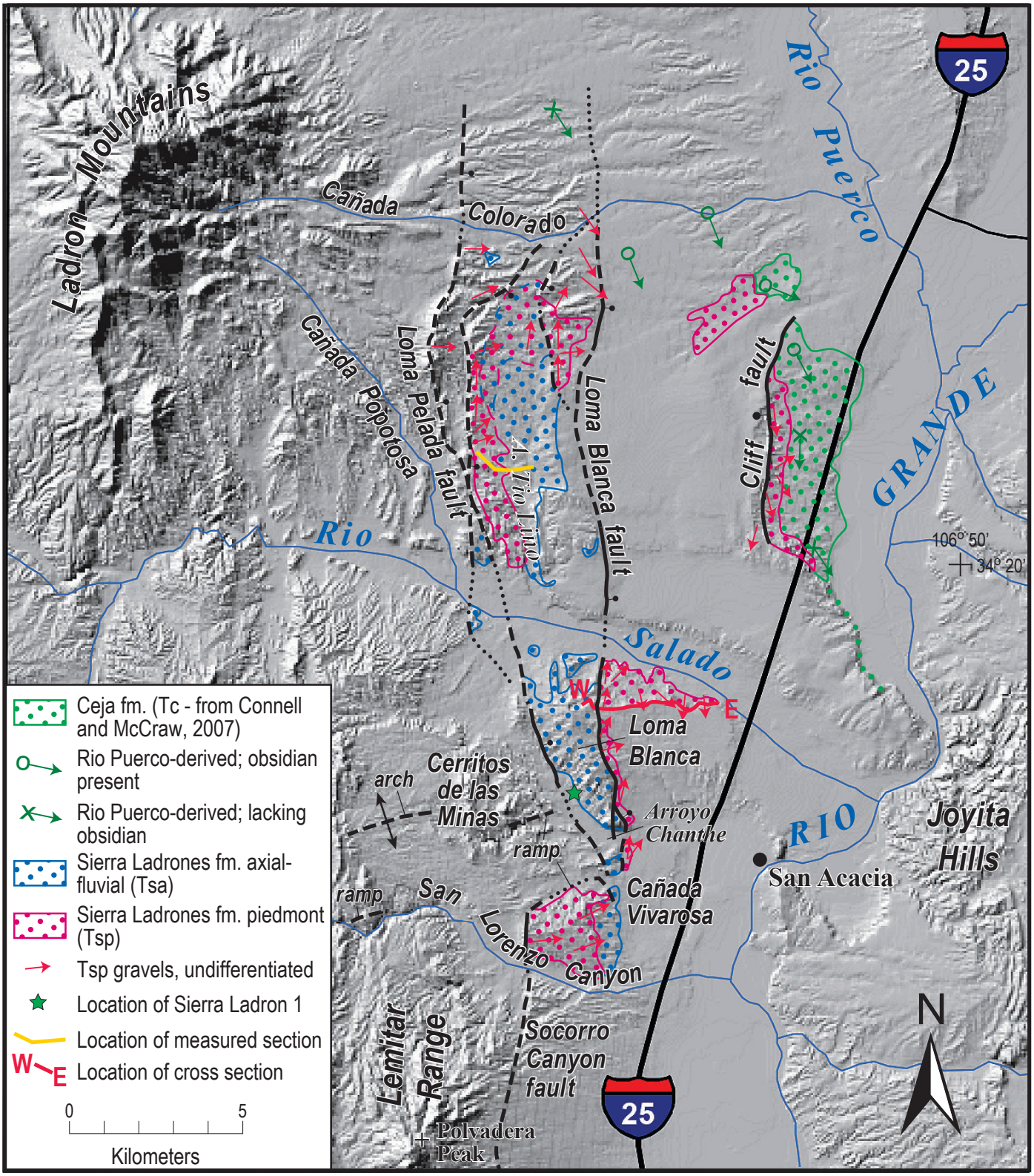

FIGURE 2. Map showing the distribution of axial-fluvial (Tsa) and piedmont alluvial (Tsp) sediment in the study area (study area shown in Fig. 1), shown on a shaded relief base map (10 m DEM, NAD 83). Star marks location of the detrital sanidine sample "Sierra Ladron 1" within the fluvial facies of the ancestral Rio Grande on the west side of Loma Blanca. Yellow line shows location of measured section of Sierra Ladrones by Connell and Lucas (2001). E-W red line shows location of cross section of Figure 5. Red arrows indicate generalized flow directions within Tsp. Green arrows with a "+" origin indicate flow directions of Rio Puerco gravel without obsidian pebbles. Green arrows with an "o" origin indicate flow directions of Rio Puerco gravels with 3.5 Ma Grants obsidian pebbles from eruptions northeast of Grants, New Mexico.

Miocene-Pliocene deposits depicted on Fig. 2). Exposures of this axial-fluvial deposit, which we designate Tsa (Figs. 2, 3), and the interfingering piedmont alluvial beds (Tsp) are exclusively between the normal, north-trending, down-to-the-east Loma Pelada and Loma Blanca faults, except at the southern exposures, where the west-side bounding fault is the Socorro Canyon fault (Fig. 2). Machette (1978) and Connell and Lucas (2001) recorded pebble imbrications and channel configurations indicating south and southeast paleoflow in the fluvial sediment. Connell and Lucas (2001) found a pumice pebble on Loma Blanca Tsa that is geochemically and age-equivalent to the Peralta Tuff (6.81–7.02 Ma; Chamberlin and McIntosh, 2007). Machette (1978) mapped Tsp on both sides of the Cliff fault along the west side of the Rio Grande Valley and thought that it consisted of piedmont deposits from the Joyita Hills. Investigations by Celep (2017; Love et al., this volume) show that this deposit is a combination of Rio Puerco and Rio Salado channel fills, overbank sediment, and fine-grained basin floor deposits with flow directions southeastward toward the Joyita Hills, where the ancestral Rio Grande was at the time. In their mapping, Connell and McCraw (2007) lumped the interfingering Rio Puerco–Rio Salado deposits as part of the Ceja Formation (Tc of Fig. 2). The Rio Puerco sediment fits the definition of the Ceja Formation, which Connell (2008) described as a widespread fluvial fan of the Rios Puerco and San Jose deposited across the western half of the Albuquerque Basin. The upper part of these interfingering Rio Puerco–Rio Salado deposits include pebbles of the 3.5 Ma obsidian from the Grants area, located approximately 127 km to the northwest of the study area (Goff and Shackley, 2022; cf. Young and Love, 2016). Geologic mapping documents a southward course of the Pliocene Rio Grande (~3 Ma) between the southern Albuquerque and the northern Socorro Basins, continuing past the western base of the Joyita Hills and into the east side of the Socorro Basin (Morgan et al., 2008; Love et al., this volume).

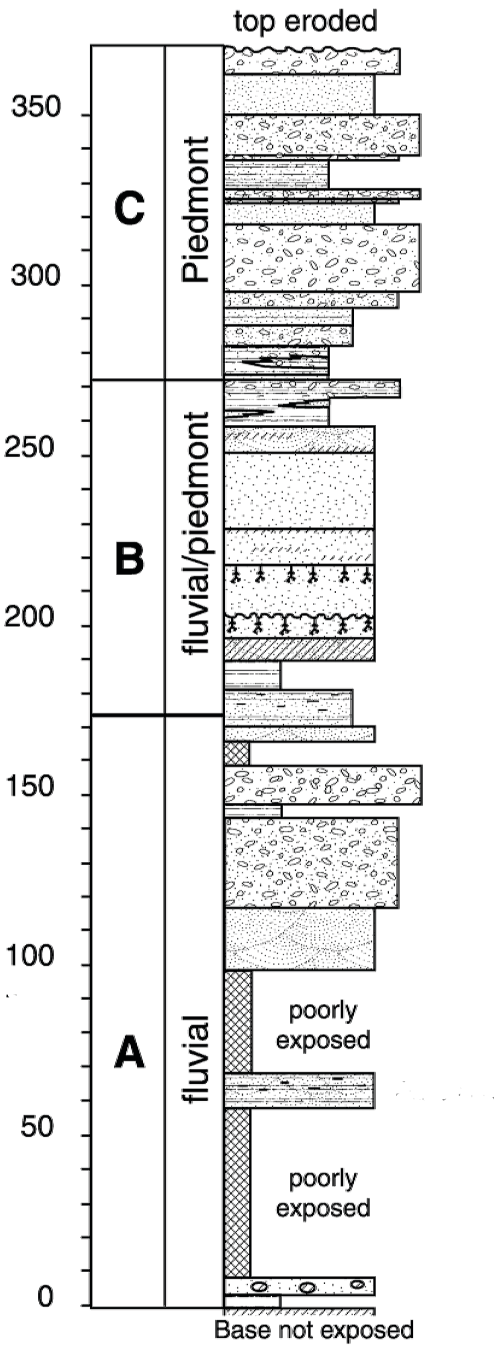

FIGURE 3. Connell and Lucas' (2001) measured section of the Sierra Ladrones Formation from the lowest exposures along Tio Lino Arroyo to the eroded top near the Loma Pelada fault (Fig. 2). As shown, piedmont alluvium increases up-section, perhaps in part due to the fact that the preserved section slopes up to the west toward the Loma Pelada fault. Nonetheless, the fluvial, well-sorted sand and pebbly sand units are interbedded with the piedmont alluvium near the top of exposures, indicating that this area was near the lowest part of the river basin during deposition.

The concept (i.e., deposits postdating the arrival of the Rio Grande in basins of the Rio Grande rift) and appellation of Sierra Ladrones Formation has been applied to related deposits in the Albuquerque and Socorro Basins, and even farther north and south along the Rio Grande rift, and has been correlated to other ancestral Rio Grande and related piedmont deposits from northern New Mexico and Colorado to Chihuahua, Mexico (Hawley, 1978; Connell et al., 2005; Repasch et al., 2017). We limit this article to the older Sierra Ladrones Formation deposits near the type area. Here, we include the ancestral Rio Salado deposits with the Sierra Ladrones Formation; note that the Sierra Ladrones–Ceja contact can locally be difficult to map due to complex interfingering of the Rio Salado and Rio Puerco deposits.

RIFT BASIN BOUNDARIES, MAJOR RIFT FAULTS, AND RIFT-MARGIN UPLIFTS IN CENTRAL NEW MEXICO

The boundary between the southern end of the Albuquerque Basin and the northern end of the Socorro Basin is delineated as a gravity high and a shallow east-northeast-trending accommodation zone (Fig. 1; Celep, 2017; Sion et al., 2020; see Appendix 1 for our justification of basin boundaries). Chamberlin et al. (2016) interpreted this zone as an arch or series of northeast-trending arches following a trend in underlying Proterozoic crustal rocks. The southeast side of the trend is reflected in at least three ramps between major north-south rift faults that cross the arches from the north, but step dextrally to

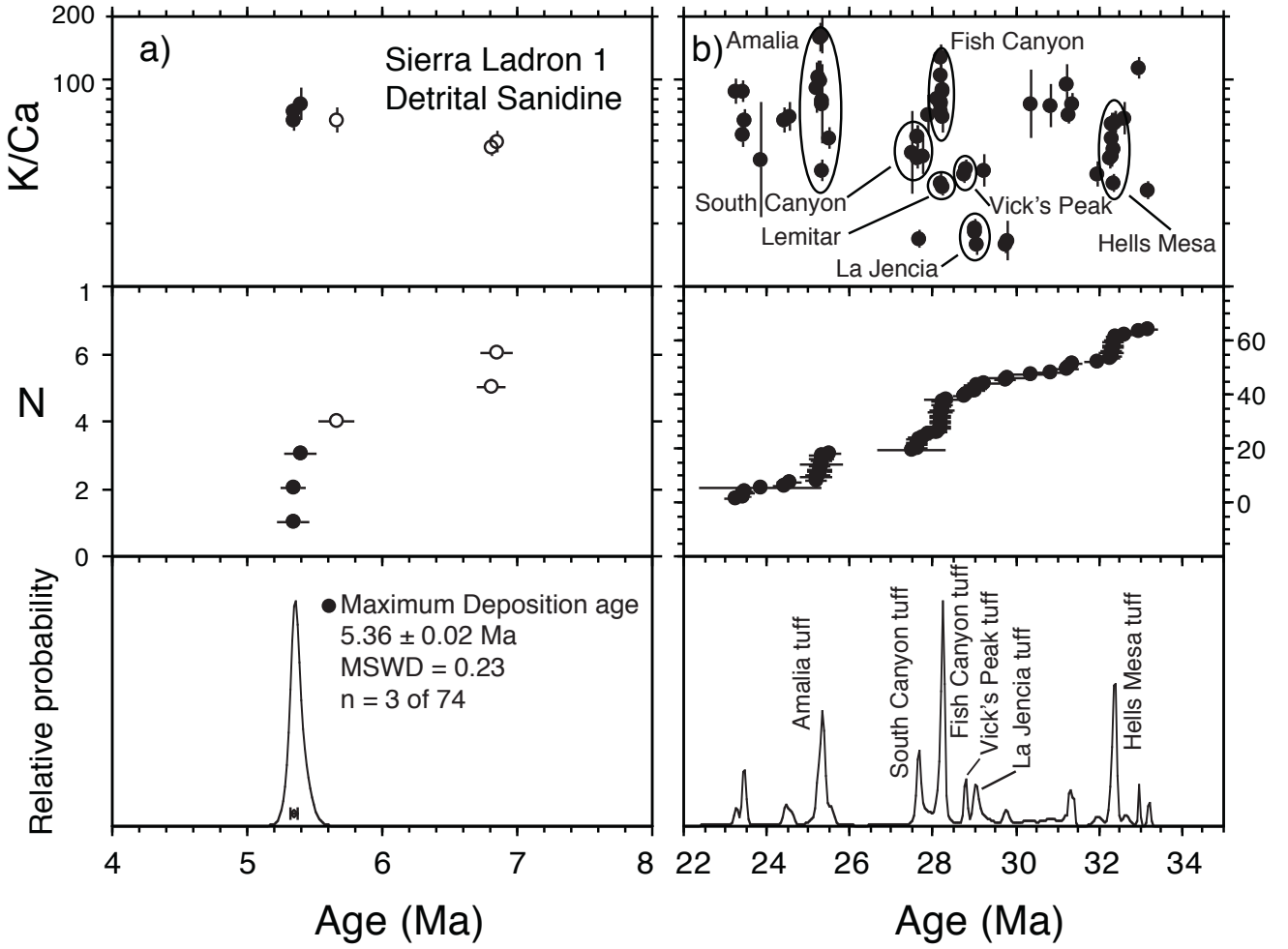

FIGURE 4. Detrital sanidine age probability diagram and associated K/Ca values for sample Sierra Ladron 1 (UTM NAD 83 13S 320577 E, 3794224 N). (a) Distribution of detrital sanidine grains with ages between 4 Ma and 8 Ma. The three youngest grains define a normal distribution and yield a maximum deposition age of 5.36±0.02 Ma. (b) The detrital sanidine distribution is dominated by grains with ages between ~23 Ma and 33 Ma, with several discrete age modes. Based on age and K/Ca values, these modes can be correlated to individual ignimbrites from various volcanic fields. Prominent age modes are identified on the probability distribution diagram.

the west along the ramps (Chamberlin et al., 2016; Figs. 1, 2). Both Grauch and Connell (2013) and Chamberlin et al. (2016) estimate the thickness of sedimentary deposits across the basin divide/arch as about 500 m.

As previously indicated, the axial-fluvial facies of the type Sierra Ladrones Formation is exposed exclusively between the down-to-the-east normal Loma Pelada and Loma Blanca faults in this area. These faults may be traced from the west side of the Albuquerque Basin south, where they cross the divide between the Albuquerque and Socorro Basins (Figs. 1, 2). In the Albuquerque Basin, northeast of the Ladron Mountains, the Loma Pelada and Loma Blanca faults lack surface manifestation on Quaternary surfaces (Machette and McGimsey, 1983). East of the Ladron Mountains, the faults splay into several strands and at least one northeast-trending fault connects the two faults south of Cañada Colorado (Fig. 2; Connell and McCraw, 2007). Here, fault scarps are preserved on select Quaternary surfaces (Machette and McGimsey, 1983; U.S. Geological Survey, 2022), but their fault histories have not been studied in detail in that area.

South of the Rio Salado, the Loma Blanca fault locally splits into several diverging and converging strands, commonly east of the main fault, and the main fault swings slightly to the southeast around the south end of Loma Blanca before continuing south to Cañada Vivarosa.

The Loma Blanca fault at the south end of Loma Blanca at Arroyo Chanthe, southeast of the Sierra Ladron 1 sample locality (Fig. 2), has two strands. The western strand offsets Tsa exclusively (Machette, 1978), and here a long-term (past 400 ka) fault rupture frequency was interpreted (Williams et al., 2017, 2019), based on U-series dating of renewed calcite growth in fractures. The newly located eastern strand (this study) veers southeast around the eastern side of the hill and has hanging wall Tsp cemented along the damage zone. At the south end, the two faults nearly converge at the east end of a 070°-striking, south-dipping inter-fault ramp and ENE-striking faults that collectively act to transfer extensional strain to the east-down Socorro Canyon fault (Figs. 1, 2).

A NEW AGE ESTIMATE OF SIERRA LADRONES FLUVIAL SAND

The base of the axial river deposits is not exposed anywhere along its outcrop belt in this area. Connell and Lucas (2001; Fig. 3) measured a 370 m thick section in Machette's proposed type area between the Loma Blanca and Loma Pelada faults (location shown in Fig. 2). The top of the axial-fluvial facies interfingers with piedmont alluvium derived from the west and south. The highest tongue of fluvial sands in this interfingering zone, located on the hanging wall of the Loma Pelada fault, is uplifted 65 m above the surface of maximum aggradation of the early Pleistocene Rio Grande fluvial deposits in the southern Albuquerque Basin 10 km to the east. Loma Blanca exposes at least 70 m of axial-fluvial facies.

Detrital sanidine $^{40}Ar/^{39}Ar$ geochronology was conducted on a sample (Sierra Ladron 1, UTM NAD 83 13S 320577 E, 3794224 N) from near the base of exposures of axial cross-bedded sands of the ancestral Rio Grande from Arroyo Chanthe on the west side of Loma Blanca (Fig. 2). Seventy-four individual grains were dated and range from ~5.32 to 547 Ma (Table 1). The youngest three grains yield a weighted mean age of 5.36±0.02 Ma that represents the maximum depositional age. This age potentially represents a source from the Jemez Mountains, because Goff et al. (2021) report an age of 5.381±0.004 Ma of the Upper Guaje rhyodacite from the Sierra de los Valles of the Jemez Mountains volcanic field. Goff et al. (2021) also report several sanidine ages between ~5.0 Ma and 3.5 Ma for this same area, however these are not represented in the detrital sanidine record. Although not conclusive, the lack of these younger sanidines may strengthen an argument that the 5.36 Ma maximum depositional age is perhaps close to the approximate depositional age of sample Sierra Ladron 1 (Fig. 4a). Thus, it is possible that the interfingering and overlying Tsp strata are younger than 5.36 Ma and perhaps older than 5.0 Ma. The 6.8 Ma grains may be related to the Peralta Tuff (cf. Chamberlin and McIntosh, 2007; Kelley et al., 2013). The detrital sanidine age distribution is dominated by ~25 to 34 Ma grains with distinct modes that can be linked to individual ignimbrites (Fig. 2b). The mode near 25.4 Ma are Amalia Tuff grains derived from the Questa caldera located in the Latir Mountains near Taos, NM. Mogollon-Datil volcanic field ignimbrites such as South Canyon, Vicks Peak, La Jencia, and Hells Mesa tuffs appear to form the modes between ~26.5 Ma and 34.3 Ma. A strong mode at 28.2 Ma is interpreted to be derived mostly from the Fish Canyon Tuff, with potential contributions from the Lemitar Tuff (Fig. 4b). Both the Fish Canyon and Lemitar tuffs are 28.2 Ma, however their sanidine K/Ca values are ~70 and ~25, respectively, allowing their identification. Both of these K/Ca values are represented in the 28.2 Ma detrital sanidine mode (Fig. 4b) and likely indicate that both tuffs are present, however a small portion of Fish Canyon sanidine grains do have lower K/Ca values related to plagioclase inclusions. The Fish Canyon Tuff mode could have implications for the evolution of the ancestral Rio Grande. If these grains are derived directly from the San Juan Mountains, it could support initial integration of the ancestral Rio Grande containing east-central San Juan Mountain headwaters (near Creede, Colorado) to the Socorro area as early as 5 Ma, as suggested by Repasch et al. (2017). Alternatively, the Fish Canyon Tuff grains could have been transported from the southernmost San Juan Mountains (New Mexico–Colorado border near Chama)

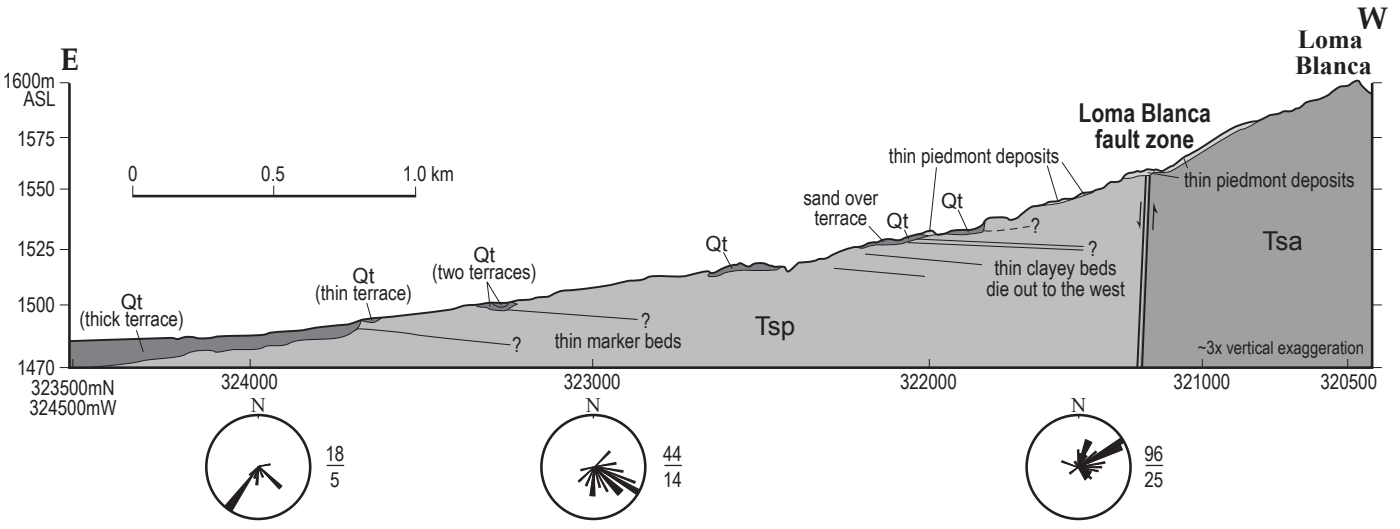

FIGURE 5. East-west profile and simplified cross section along the southern rim of the Rio Salado Valley between Loma Blanca and a thick Rio Salado terrace that overlies eroded Tsp. UTM Easting coordinates labeled on x-axis (NAD 83, 13 S), but the 1 km intervals are slightly affected by the cross section following the valley rim. The predominantly fine-grained marker beds have apparent west dips in the line of the section and pinch out to the west, toward the Loma Blanca fault zone. The rose diagrams along the bottom of the cross section show pebble imbrications and channel-margin directions of the few conglomerates found in the section. The numbers adjacent to the diagrams show the number of observations in the numerator and the number of conglomerate locations in the denominator. Note that the rare, easternmost, and lowest conglomerates were transported predominantly to the south, southeast, and southwest. The conglomerates in the central part of the section exhibit transport predominantly to the southeast, with some transport to the southwest and northeast. The more abundant transport directions closest to the fault are predominantly to the northeast. Note several levels of terraces deposited by the paleo–Rio Salado after an unknown amount of Tsp was eroded. Not shown are several minor (~6–7 m vertical displacement) northwest-trending faults cutting Tsp and at least the lowest terrace to the east.

TABLE 1. Detrital sanidine $^{40}Ar/^{39}Ar$ analytical data for sample Sierra Ladron 1.

	ID	$^{40}Ar/^{39}Ar$	$^{38}Ar/^{39}Ar$	$^{37}Ar/^{39}Ar$	$^{36}Ar/^{39}Ar$ (x 10^{-3})	$^{39}Ar_K$ (x 10^{-15} mol)	K/Ca	$^{40}Ar^*$ (%)	Age (Ma)	±1σ (Ma)
Sierra Ladron1, DetritalSanidine, J=0.0037789±0.02%, NM-289F, Lab#=65516										
	06	0.8524	0.0129	0.0082	0.2372	2.328	62.0	91.8	5.352	0.054
	03	0.8221	0.0129	0.0075	0.1337	4.302	68.3	95.2	5.354	0.028
	36	0.8332	0.0129	0.0068	0.1481	1.886	74.8	94.8	5.400	0.065
x	31	1.094	0.0130	0.0081	0.8990	1.896	62.8	75.6	5.670	0.069
x	26	1.046	0.0147	0.0111	0.1711	3.194	46.0	95.2	6.826	0.039
x	24	1.131	0.0130	0.0104	0.4387	2.784	49.0	88.5	6.862	0.045
x	17	3.444	0.0132	0.0060	0.1712	2.325	85.1	98.5	23.270	0.053
x	23	3.440	0.0128	0.0060	0.0795	3.937	85.3	99.3	23.432	0.032
x	13	3.480	0.0132	0.0096	0.1968	2.163	53.3	98.3	23.466	0.056
x	25	3.458	0.0128	0.0082	0.1185	3.502	62.3	99.0	23.478	0.036
x	27	4.081	0.0095	0.0128	2.022	0.097	39.9	85.4	23.9	1.2
x	02	3.732	0.0131	0.0082	0.5612	2.592	62.4	95.6	24.451	0.050
x	41	3.752	0.0135	0.0078	0.5661	1.919	65.3	95.5	24.580	0.066
x	07	3.906	0.0132	0.0019	0.7631	3.531	273.4	94.2	25.227	0.038
x	30	4.173	0.0142	0.0058	1.663	0.864	88.7	88.2	25.24	0.15
x	35	3.775	0.0130	0.0050	0.2917	2.180	101.3	97.7	25.291	0.058
x	15	3.718	0.0131	0.0016	0.0834	1.715	313.3	99.3	25.316	0.072
x	28	3.780	0.0134	0.0053	0.2890	1.532	97.0	97.7	25.328	0.080
x	10	3.802	0.0131	0.0033	0.3619	3.985	156.6	97.2	25.329	0.033
x	27	4.005	0.0140	0.0068	1.033	0.425	75.1	92.4	25.36	0.29
x	30	4.012	0.0130	0.0066	1.054	3.606	76.8	92.2	25.368	0.039
x	05	3.758	0.0129	0.0143	0.1964	2.185	35.8	98.5	25.371	0.055
x	06	3.822	0.0130	0.0032	0.4059	2.425	159.2	96.9	25.376	0.051
x	19	3.759	0.0133	0.0101	0.1073	2.014	50.5	99.2	25.551	0.061
x	35	4.244	0.0144	0.0118	0.7619	0.203	43.2	94.7	27.54	0.59
x	37	4.057	0.0129	0.0125	0.0835	2.527	41.0	99.4	27.637	0.049
x	21	4.139	0.0131	0.0098	0.3444	3.607	52.0	97.6	27.664	0.036
x	02	4.065	0.0128	0.0098	0.0916	2.647	52.0	99.4	27.669	0.046
x	33	4.293	0.0127	0.0309	0.8605	1.437	16.5	94.1	27.688	0.087
x	22	4.158	0.0140	0.0123	0.3503	0.875	41.5	97.5	27.78	0.14
x	26	4.132	0.0136	0.0077	0.1909	0.952	66.0	98.6	27.93	0.13
x	18	4.147	0.0130	0.0065	0.1503	2.296	79.0	98.9	28.110	0.053
x	34	4.156	0.0131	0.0074	0.1358	2.469	68.9	99.0	28.203	0.050
x	33	4.145	0.0126	0.0050	0.0951	2.945	103.0	99.3	28.207	0.042
x	17	4.237	0.0130	0.0069	0.4011	2.844	73.9	97.2	28.219	0.045
x	11	4.324	0.0131	0.0041	0.6922	3.841	125.9	95.3	28.224	0.036
x	22	4.155	0.0129	0.0067	0.1152	6.537	76.4	99.2	28.233	0.020
x	28	4.147	0.0128	0.0067	0.0889	3.528	76.0	99.4	28.236	0.035
x	31	4.186	0.0132	0.0165	0.2194	1.956	31.0	98.5	28.240	0.064
x	32	4.246	0.0125	0.0079	0.4177	1.328	64.6	97.1	28.247	0.093
x	05	4.221	0.0129	0.0058	0.3272	7.246	87.8	97.7	28.256	0.019
x	24	4.161	0.0129	0.0060	0.1243	2.493	84.8	99.1	28.259	0.049
x	04	4.164	0.0129	0.0173	0.1261	6.873	29.4	99.1	28.280	0.018
x	04	4.715	0.0136	1.008	2.229	0.408	0.51	87.7	28.35	0.31
x	20	4.243	0.0129	0.0150	0.1461	3.818	33.9	99.0	28.773	0.033
x	10	4.252	0.0130	0.0140	0.1612	3.562	36.3	98.9	28.806	0.036
x	19	4.292	0.0131	0.0270	0.1925	2.380	18.9	98.7	29.025	0.053
x	08	4.272	0.0132	0.0281	0.1167	1.777	18.2	99.2	29.040	0.069
x	29	4.297	0.0131	0.0323	0.1804	1.246	15.8	98.8	29.083	0.099
x	09	4.444	0.0133	0.0144	0.5890	0.744	35.4	96.1	29.25	0.16
x	20	4.403	0.0132	0.0326	0.2036	1.938	15.7	98.7	29.761	0.064
x	13	5.172	0.0140	0.0312	2.782	0.259	16.4	84.1	29.81	0.49

TABLE 1. (continued)

	ID	$^{40}Ar/^{39}Ar$	$^{38}Ar/^{39}Ar$	$^{37}Ar/^{39}Ar$	$^{36}Ar/^{39}Ar$ (x 10^{-3})	$^{39}Ar_K$ (x 10^{-15} mol)	K/Ca	$^{40}Ar^*$ (%)	Age (Ma)	±1σ (Ma)
x	11	4.882	0.0139	0.0069	1.512	0.436	74.2	90.8	30.38	0.28
x	16	4.598	0.0135	0.0070	0.3031	0.817	73.3	98.1	30.87	0.15
x	09	4.594	0.0136	0.0055	0.1074	1.428	92.9	99.3	31.234	0.087
x	12	4.651	0.0129	0.0077	0.2703	8.005	66.0	98.3	31.296	0.017
x	07	4.641	0.0129	0.0068	0.1934	4.719	74.5	98.8	31.382	0.027
x	08	4.868	0.0128	0.0150	0.6668	1.248	34.1	96.0	31.983	0.098
x	18	4.756	0.0129	0.0125	0.1358	2.364	40.7	99.2	32.286	0.052
x	12	4.822	0.0130	0.0100	0.3409	3.126	51.1	97.9	32.324	0.042
x	38	4.760	0.0129	0.0123	0.1235	1.582	41.5	99.3	32.334	0.078
x	16	4.835	0.0130	0.0085	0.3686	3.631	59.7	97.8	32.354	0.036
x	03	4.914	0.0130	0.0112	0.6296	3.338	45.5	96.2	32.365	0.041
x	01	4.833	0.0130	0.0085	0.3465	3.870	60.1	97.9	32.381	0.034
x	14	4.772	0.0128	0.0167	0.1447	5.604	30.6	99.1	32.382	0.023
x	29	4.777	0.0129	0.0084	0.1432	2.816	60.6	99.1	32.409	0.044
x	01	4.820	0.0128	0.0083	0.2874	4.433	61.4	98.2	32.412	0.029
x	14	4.941	0.0132	0.0081	0.5804	1.421	63.2	96.5	32.647	0.089
x	32	4.852	0.0129	0.0046	0.1182	5.918	110.3	99.3	32.968	0.022
x	15	4.899	0.0128	0.0178	0.1630	3.654	28.7	99.0	33.206	0.034
x	39	5.726	0.0135	0.0070	0.6743	0.780	73.2	96.5	37.78	0.16
x	34	11.87	0.0127	0.0089	0.9960	1.492	57.1	97.5	78.293	0.091
x	21	92.13	0.0128	0.0015	0.0909	1.599	330.3	100.0	546.65	0.43
	MDA±2σ		**n=3**		**MSWD=0.23**				**5.36**	**0.02**

Notes:
Isotopic ratios corrected for blank, radioactive decay, and mass discrimination, not corrected for interfering reactions.
Errors quoted for individual analyses include analytical error only, without interfering reaction or J uncertainties.
Mean age is weighted mean age of Taylor (1982). Mean age error is weighted error of the mean (Taylor, 1982), multiplied by the root of the MSWD where MSWD>1, and also incorporates uncertainty in J factors and irradiation correction uncertainties.
Isotopic abundances after Steiger and Jäger (1977).
x preceding sample ID denotes analyses excluded from mean age calculations.
Ages calculated relative to FC-2 Fish Canyon Tuff sanidine interlaboratory standard at 28.201 Ma.
Decay Constant (LambdaK (total)) = 5.463e-10/a
Correction factors:
$(^{39}Ar/^{37}Ar)_{Ca}$ = 0.0006756±0.000001
$(^{36}Ar/^{37}Ar)_{Ca}$ = 0.000266±0.0000003
$(^{40}Ar/^{39}Ar)_{K}$ = 0.00812±0.0001

by the Chama River, thereby negating the need to have a direct ancestral Rio Grande connection to the east-central San Juan Mountains during Rio Grande deposition at Arroyo Chanthe. There are multiple large ignimbrites in the San Juan volcanic field that range in age from about 27 to 37 Ma (Lipman, 2007), and these ignimbrites do not appear to be part of the detrital sanidine distribution for the Sierra Ladron 1 sample. This may indicate that the Fish Canyon Tuff crystals were not derived from outcrops in Colorado, but rather derived from the Tusas Mountains in northern New Mexico. Zimmerer and McIntosh (2011) dated sanidine from the Las Tablas Tuff at 28.28±0.07 Ma near the southeastern boundary of the San Luis Basin and suggested that this tuff could be a distal outflow of the Fish Canyon Tuff that erupted from the La Garita Caldera in Colorado. Therefore, the lack of a more extensive distribution of San Juan Mountain volcanic field ignimbrites, coupled with the strong mode of Amalia Tuff grains, suggests that the 28.2 Ma detrital sanidine grains may have been derived from northern New Mexico rather than Colorado.

PEBBLE TRANSPORT DIRECTIONS OF SIERRA LADRONES ALLUVIAL FACIES

The southern (for this article; Fig. 2) exposures of piedmont deposits (Tsp) east of the Socorro Canyon fault and north of the San Lorenzo drainage consist of pebble, cobble, and boulder conglomerate, pebbly sandstone, and thin, reddish-brown beds of silt and clay (Chamberlin et al., 2001). Transport directions of the large clasts are generally to the east and northeast. The Tsp strata north of the San Lorenzo drainage overlie conformably the fluvial sands of the ancestral Rio Grande (Tsa), and both dip to the west about 10–20° toward the Socorro Canyon fault. This geometry, and the mapped pattern of Tsp (Chamberlin et al., 2001), suggests that Tsp is 410–750 m thick. Clasts in the Tsp conglomerates include cobbles of reddish-brown gravel reworked from outcrops of basal Popotosa volcanic-clast conglomerate exposed on the western slopes of the Lemitar Range to the southwest. It should be noted that 23–24 km farther south, near the mouth of Socorro Canyon, at a similar elevation east of and offset by the Socorro Canyon fault, is a

similar sequence of piedmont gravel overlying ancestral Rio Grande sand, in turn overlain by a 3.78 Ma basalt flow that came down the ancestral Socorro Canyon (Chamberlin, 1999). Overlying that flow are more gravels from the Socorro Canyon drainage. This sequence may provide an indication of the age of Tsp and consequently would suggest a regional piedmont progradation occurred ca. 4–5 Ma following aggradation of the ancestral Rio Grande.

Limited exposures of Tsp between Cañada Vivarosa and Arroyo Chanthe, on the southern edge of the San Acacia quadrangle (Machette, 1978), are restricted to the hanging wall of the Loma Blanca fault. They consist of reddish-brown sandstones, silt-clay beds, and thin pebble conglomerates. The conglomerates have imbrications that indicate that paleoflow was to the north and northeast. The small pebbles consist of at least 70% volcanic clasts, many of which have reddish-brown clay coatings similar to the reworked clasts of the Popotosa conglomerates observed in Sierra Ladrones piedmont deposits near San Lorenzo Canyon.

The most extensive southern exposures of Tsp are adjacent to the Loma Blanca fault between Arroyo Chanthe and the Rio Salado and lie in the hanging wall (W-E cross section of Fig. 2; Fig. 5). The unit commonly dips 4–6° westward or northwestward toward the fault. Gravel found in the well-cemented damage zone consists primarily of Tsp clasts of the hanging wall. The cement in Tsp conglomerates is commonly calcium carbonate, but locally includes manganese-iron oxides and hydroxides; silica is present in rare outcrops. Facies of Tsp change eastward between the predominantly light reddish-brown sand and thin pebble conglomerates (within about half a kilometer east of the fault) to increasingly abundant interfingering tongues of reddish-brown silty clay and pale reddish-brown sand (Fig. 5). The exposures east of UTM 323200 E dip 2–4° to the north-northwest.

Conglomerates close to the fault show transport primarily to the northeast (ranging from north to southeast), whereas conglomerates, pebbly channels, and channel margins farther east show a variety of orientations but are mainly southeast (Fig. 5). The rare pebble conglomerates farthest to the east and lowest in the stratigraphic section show transport to the southeast or south-southwest (Fig. 5). Some distinctive beds (commonly reddish-brown or brown and composed of clay or pedogenic carbonate horizons) along the exposures may be traced westward, where they pinch out into more massive pebbly sand. Exposed thickness close to the fault is about 48 m, and composite thickness of the finer-grained interfingering beds to the east is about 55 m. Shallow holes drilled in the hanging wall adjacent to the Loma Blanca fault (Hinojosa, 2021) yield 30 m more of Tsp but do not show its base. At the top of hanging-wall exposures located ~1 km south of the W-E line on Figure 2 lie coarse cobble and pebble gravel derived from Cerritos de las Minas to the southwest. This gravel had to have been transported northeastward across the Loma Pelada fault and across the fluvial sands at Loma Blanca before they were down-faulted at least 70 m in the hanging wall. This implies at least 155 m of offset (70 m below top of Loma Blanca plus 55 m of exposed thickness plus >30 m of borehole thickness). Nowhere along the exposures of Tsp are there any clasts from the Tsa sands, pebbly sandstones, or clasts of fossil wood derived from the footwall of the fault. Along the southern rim of the Rio Salado Valley is a flight (set of terraces having unique heights above modern stream grade) of Rio Salado coarse-gravel terraces capping exposures of Tsp. These terraces are overlain by younger sandy "piedmont" alluvium and blocks of sandstone and fossil wood derived from the footwall Tsa.

North of the Rio Salado, along the west, east, and north drainage divides of Tio Lino Arroyo (Figs. 2, 3), exposures of Tsa interfinger up section with Tsp (Connell and Lucas, 2001). Connell and McCraw (2007) mapped paleoflow based on imbrication directions in tongues of pebble-cobble gravel of the non-fluvial, piedmont alluvium that show paleotransport to the north and northeast (Fig. 2). Further investigation by the authors showed that some of the imbrications also show transport to the east, and clast compositions indicate that some channels transported Proterozoic pebbles and cobbles from the Ladron Mountains, whereas other gravels of volcanic, sedimentary, and Proterozoic rocks are similar to those from the south side of the Rio Salado. The highest part of the drainage divide on the west side of Tio Lino Arroyo, which lies on the hanging wall of the Loma Pelada fault, exposes cobbles and small boulders of rounded mixtures of volcanic rocks, limestone, and sandstone, and Proterozoic crystalline rocks transported to the north. These sediments must have been derived from a different, larger-clast-producing source than the pebble gravels farther south, perhaps an ancestral Rio Salado (Love et al., 2017). Stratigraphically overlying, and perhaps incised into, these Tsp deposits are eastward-shed coarse subangular boulders and cobbles of Proterozoic quartzite and other metamorphic rocks derived from the Ladron Mountains.

The eastern drainage divide of Tio Lino Arroyo consists of down-dropped, relatively small, arcuate fault blocks (too detailed to be shown in Fig. 2) bounded on the east side by the Loma Blanca fault (Connell and McCraw, 2007). These blocks preserve interfingering of fluvial sand and piedmont alluvium. The alluvium has small, gravelly channel fills showing predominantly northward-to-northeastward paleotransport (Connell and McCraw, 2007), with a few channels trending to the east. Correlative alluvial channel deposits with northeast transport directions exposed on one of these fault blocks are also exposed on the next small fault block to the north. Above them, similar to stratigraphically high deposits on the west side of Tio Lino, are eastward-shed piedmont deposits from the Ladron Mountains.

In the next fault-bounded block to the north and west of the Loma Blanca fault, located between Cañada Colorado and about 1.4 km south of that drainage, Connell and McCraw (2007) and our observations show alluvial channels oriented to the southeast with pebble imbrications showing transport to the southeast. These gravels are similar in composition to Tsp transported to the north and northeast exposed on the previously discussed block to the south (near Arroyo Tio Lino). These Tsp deposits are overlain by inset Pleistocene piedmont gravel of Proterozoic cobbles and boulders derived from the Ladron Mountains.

Three km (2 mi) north of Cañada Colorado, on the edge of exposures on the footwall of the Loma Blanca fault in the farthest north Rio Puerco paleoflow indicator on Figure 2, Connell and McCraw (2007) mapped a small exposure of ancestral Rio Puerco pebbly sand and gravel belonging to the Ceja Formation. Flow directions in that deposit are generally to the south-southeast. No clasts of the 3.5 Ma obsidian from the Grants area (Love and Young, 1983; Young and Love, 2016; cf. Goff and Shackley, 2022) were found in these pebbly sand beds. However, exposures on the hanging wall of the Loma Blanca fault to the east also have gravel channels of the ancestral Rio Puerco, which as a depositional unit has been traced southward across the southwestern Albuquerque Basin by Love and Young (1983). These gravels contain pebbles of Grants obsidian. Similar gravels containing both the obsidian (Young and Love, 2016) and Blancan fossil vertebrates (Morgan et al., 2009) underlie the Llano de Albuquerque, the highest fill of the southwestern Albuquerque Basin (McCraw, 2016). To the southeast of Cañada Colorado, on both sides of the Cliff fault, coarse sub-angular gravels from the ancestral Rio Salado interfinger with pebble gravels of the Rio Puerco (Celep, 2017; Love et al., this volume). Upper exposures at the northern end of the Cliff fault include obsidian from the Grants area.

DISCUSSION

In the Arroyo Tio Lino area and south of Rio Salado, transport directions of Tsp overlying Tsa and Tsp on the hanging wall of the Loma Blanca fault are generally to the north and northeast (Fig. 2). These Tsp paleoflow directions are opposite the southward gradient of the ancestral Rio Grande (Machette, 1978; Connell and Lucas, 2001). This implies that either the southwestern edge of the Albuquerque Basin became tilted to the north along north-trending faults or that uplift of the Lemitar Range, its northern extension, and Cerritos de las Minas, all west of the Loma Pelada fault, shed large amounts of reworked Miocene Popotosa sediments to the north and northeast across the traces of both the Loma Pelada and Loma Blanca faults. Northward progradation of these alluvial sediments, if they were thick and extensive enough, may have diverted the ancestral Rio Salado to the north and northeast as well.

On the south side of the Rio Salado, an interesting trend in paleoflow directions occurs on the hanging wall of the Loma Blanca fault (Fig. 5). At paleoflow sites located ~2.5 km and 1.5 km east of the fault (left and central rose diagrams, Fig. 5), there is an up-section trend in paleoflow. Lowest exposures are interpreted to be distal piedmont to basin-floor facies and exhibit southwest to southeast paleoflow directions. Gravel channel fills become slightly more common up-section in exposures 1.5 km east of the fault (central rose diagram, Fig. 5), where paleoflow data show more southeasterly trends. Exposures of Tsp within 0.5 km east of the Loma Blanca fault predominantly show northeast-directed transport of the coarser, pebbly sand facies at all stratigraphic levels. It might be expected that the first Tsp to overlie the fluvial sand of Tsa would show southerly transport directions, perhaps reflected in the eastern Tsp of Figure 5. The diverse directions of the middle part of Tsp in the cross section might reflect drainages flowing southeastward off of an alluvial fan system to the northwest of the present outcrops, probably corresponding with Tsp tributaries reaching into the northern Lemitar Mountains. The north and northeast transport of pebbly sand and pebble conglomerates of Tsp adjacent to the Loma Blanca fault south of the Rio Salado may reflect deposition in paleotopographic low areas coinciding with maximum subsidence of the hanging wall adjacent to the fault, interfingering with tongues of fine-grained facies and paleosols to the east. The interfingering implies that sediment deposition in the eastern part of the unit kept pace with sedimentation along the fault. Because unit Tsp on the hanging wall contains no obvious debris from the Tsa fluvial sands of the footwall, those sands were probably not exposed along the fault at the time of hanging-wall deposition. The prograding alluvial fan from the south-southwest must have buried the fluvial sands while the Loma Blanca fault developed. This scenario would mean that as the fault developed, at least an 85 m thick sequence of Tsp pebbly sands on the hanging wall were offset at least 70 m below the top of the fluvial sands of Loma Blanca (70 m being the topographic height above Tsp on the adjacent footwall of Loma Blanca). Post-faulting erosion of the footwall and hanging wall prevents our ability to recognize the complete record of strata reworked from the footwall, to estimate original paleoscarp height, and to determine original thickness of Tsp on the footwall.

Similar predominantly northward transport may have occurred along hanging-wall paleotopographic lows along the Loma Pelada fault and smaller fault blocks between the Loma Pelada and Loma Blanca faults. Because some of the gravel channel fills are more coarse grained, particularly along the hanging wall of the Loma Pelada fault, it's possible that the Tsp fan from the south diverted the Rio Salado northward (a phenomenon that continued later and was partially documented by Celep [2017], Love et al. [2017], and Love et al. [this volume]). Many features of the small Tsp channel fills in this area, such as their clast sizes, compositions, and northerly transport on the east side of Tio Lino Arroyo, are similar to the Tsp channels farther south.

The limited Tsp exposures in the Cañada Colorado area and 3 km to the south (Fig. 2) have clast compositions similar to Tsp to the south, but they were transported to the southeast. Their location southeast of one of the cross faults between the Loma Pelada and Loma Blanca faults, and their proximity to small outcrops of ancestral Rio Puerco sediments (Tc; Ceja Formation of Connell and McCraw, 2007), may provide an explanation for their transport direction. The Rio Puerco could not have flowed southeast in this area until after the Rio Grande abandoned its course exposed to the west. Presumably the Tsp alluvium at the head of Tio Lino arroyo continued north between the two large faults (Fig. 2). If the Tsp overlying type Tsa along the hanging wall of the Loma Pelada fault extended to the north and was exposed in the footwall of one of the cross faults after the Rio Puerco established its southeastern course across the area, local reworking of Tsp into a younger piedmont deposit would create alluvium looking like the older Tsp, but could show channels and flow directions to the southeast

above ancestral Rio Puerco deposits.

The apparent highest part of the uplift of Tsa on Loma Blanca is just north of the basin divide delineated by gravity and the projected east-northeast trends of the West Mesa (west of area of Fig. 2) and Cerritos de las Minas arches (Chamberlin et al., 2016; Figs. 1 and 2); this high area is also north of the hinges of three ramps (shown on Fig. 1) related to the dextral stepovers of the major rift faults (Fig. 2; Chamberlin et al., 2016). This arch trend is also above the area of maximum uplift of the Socorro magma body (Fialko and Simons, 2001; Finnegan and Pritchard, 2009; Chamberlin et al., 2016; Axen et al., 2019). With the revelation that multiple magma bodies have been emplaced over the past 1–3 million years (Reiter et al., 2010), the uplift of Loma Blanca could be due to a combination of thermal expansion above the magma bodies and rift-related fault offsets (including footwall uplifts). The eastern exposures of Tsp dipping north-northwest (south of the Rio Salado) and the arching of a basaltic-andesite lava flow east of San Acacia and the Cerro Indio fault (Figs. 1 and 2) may suggest that the arching trend continues to the northeast. However, much of Tsp has been eroded by the Rio Grande and its tributaries to form its present valley in the area to the south. The Quaternary terraces of the Rio Salado and Rio Grande above Tsp exposed south of the Rio Salado do not show evidence of tilting due to arching. Whether the trend of the arch appears to deflect Quaternary terraces of the Rio Grande on the west side of the Joyita Hills is controversial (Love et al., 2009; cf. Phillips and Sion, this volume). The trend of arches appears to continue to the northeast between the Joyita Hills and the southern end of the Los Pinos Mountains and may have caused widespread erosion of early Quaternary deposits (cf. Allen and Love, 2013).

The sequence of depositional episodes across the southern boundary of the Albuquerque Basin shows the interplay between tectonics and sedimentation in the area. First, the western course of the ancestral Rio Grande must have been in the lowest part of the area at the time, and our interpreted divide between the structural basins did not influence its position. Second, the subsequent northward transport of Tsp alluvium suggests that the uplift of the Lemitar Range became a major source area to furnish sediments into the southern Albuquerque Basin. Again the accommodation zone/northeast-trending arches between the two rift basins do not appear to be a major influence on transport directions across the area. Third, the Loma Pelada and Loma Blanca faults became active during the uplift of the Lemitar Range. Displacement rates along the Loma Pelada and Loma Blanca faults appear to have been relatively high, creating paleotopographic lows immediately adjacent to these faults, allowing piedmont drainages from the southwest to be deflected into these lows and furnishing sediments to a fan-distributary system that fed an interfan low between the toes of these fans and a postulated ancestral Rio Salado fan to the north. Growth of this southwest-derived fan-distributary system may have deflected the ancestral Rio Salado northward. Fourth, continued uplift of the footwalls of both the Loma Pelada and Loma Blanca faults and probably the Ladron rift-flank uplift isolated these fault blocks from the rest of the southern Albuquerque Basin. The Rio Grande shifted to the east to establish a course down the center of the Albuquerque Basin prior to 3.5 Ma. Fifth, the arrival of the Rio Puerco from the north and its dominance in aggrading the western half of the Albuquerque Basin after the Rio Grande shifted to the east may reflect its overwhelming sediment loads, easily erodible sediments in its headwaters, climate shifts, and water losses to groundwater during sediment transport. The shift in the course of the Rio Grande to the east is well established, but it is not known whether: (1) the course gradually moved eastward and underlies the area east of the Loma Blanca fault (Connell and McCraw, 2007, cross section), or (2) whether the river avulsed (stepped) eastward farther north in the basin and followed normal-fault-related hanging-wall topographic lows to the south. It seems likely that the course of the Rio Grande was influenced by offsets along the West Joyita fault near the divide between the Albuquerque and Socorro Basins.

CONCLUSIONS

Two major sedimentary facies of fluvial sand (Tsa) and piedmont alluvium (Tsp) are exposed on the southwest edge of the Albuquerque Basin and the northern Socorro Basin, between and east of the down-to-the-east Loma Pelada and Loma Blanca normal faults. The fluvial pebbly sand facies was deposited by the south-flowing ancestral Rio Grande. A detrital sanidine age determination from a sample near the base of exposures on Loma Blanca shows a maximum depositional age of 5.36 Ma. The interfingering and overlying piedmont alluvial unit Tsp exhibits north-to-northeast flow directions between the faults and immediately east of the Loma Blanca fault. The clast size, compositions, and imbrications of Tsp south of the Rio Salado suggest that the unit was derived from uplift of the Lemitar Range and Cerritos de las Minas. North of the Rio Salado, some of the Tsp alluvium is similar, but closer to the Loma Pelada fault the larger clasts and diverse compositions suggest a more competent stream and slightly different sources, and transport directions continued to be predominantly north and northeast. The northeasternmost exposures of apparent Tsp appear to be younger and related to the arrival of the Rio Puerco after the ancestral Rio Grande no longer followed the western course.

The reversal of flow directions between the south-flowing axial and north-northeast-flowing piedmont facies implies that gradients changed from south to northeast. This gradient change could either be from uplift along the northerly trend of the Lemitar Range accompanied by increases in sediment supply, causing progradation of the piedmont alluvium, or there could have been tectonic reversals of tilt into the Albuquerque Basin farther north. A combination of the two is also possible. The two facies cross the boundary area between the southern Albuquerque Basin and northern Socorro Basin and apparently were not influenced by the northeast-trending crustal feature. However, the transition between the two basins does affect the southern terminations of the Loma Pelada and Loma Blanca faults (and other rift-related, north-south faults) and the amount of uplift and erosion of the two facies, particularly at Loma Blanca. Exposures of Tsp in the hanging wall east of the Loma

Blanca fault in the area south of the Rio Salado are dropped at least 155 m and show no obvious debris shed or other sediment-related influences from erosion of fluvial facies on the footwall. This suggests that the Tsp alluvium prograded NNE across what was previously fluvial facies and also crossed the traces of the Loma Pelada and Loma Blanca faults. Tsp on top of the fluvial facies must have been thick enough on the Loma Blanca fault footwall that underlying fluvial pebbles and sand were continually buried, since no detritus from the axial-fluvial facies is seen in Tsp on the Loma Blanca fault hanging wall. This summary suggests that the contrasting sedimentology and structural evolution of the two rift basins and the transition zone deserve much more detailed study.

The age of Tsp is constrained by the new maximum depositional age of ~5.36 Ma of Tsa at Loma Blanca and may be approximately similar to the age of Tsp deposits interfingering with a basalt flow with an age of 3.78 Ma at Socorro Canyon. At the north end of our studied exposures in the Albuquerque Basin, cross-cutting relationships of Rio Puerco deposits (Ceja Formation; Tc) post-date the abandonment of the early western course of the ancestral Rio Grande. The deposits of Ceja Formation consistently are graded to the southeast toward an ancestral Rio Grande near the center of the Albuquerque Basin. Some of the Rio Puerco–related deposits predate the arrival of clasts of ~3.5 Ma obsidian from the Grants area into the southern Albuquerque Basin, whereas younger Ceja Formation deposits contain pebbles of Grants obsidian. Therefore, most of Tsp is interpreted to span 3.5 to 5.0 Ma in the study area.

ACKNOWLEDGMENTS

We thank Kathy Granillo, manager, and staff of Sevilleta National Wildlife Refuge for permission and encouragement for our research. Much of the fieldwork and accompanying research was supported by the New Mexico Bureau of Geology and Mineral Resources. We thank Mike Chavez and Gary Loos, volunteers at the refuge, for help with fieldwork. We are grateful for discussions with and written reviews by Dan Koning to clarify and extend some of the concepts we developed. We thank Dr. Fraser Goff for his communications regarding the ages of late Neogene volcanic eruptions in the eastern Jemez Mountains. We appreciated and adopted many of the suggestions and comments made by reviewers Drs. Cather and Gotee.

REFERENCES

Allen, B.D., and Love, D.W., 2013, Geologic map of the Becker SW 7.5-minute quadrangle, Socorro County, New Mexico: New Mexico Bureau of Geology and Mineral Resources, Open-file Geologic Map 233, scale 1:24,000.

Axen, G., van Wijk, J., Phillips, F., Harrison, B., Sion, B., Yao, S., and Love, D., 2019, The Socorro magma body: New Mexico Earth Matters, Winter, p. 1–5.

Cather, S.M., Chamberlin, R.M., Chapin, C.E., and McIntosh, W.C., 1994, Stratigraphic consequences of episodic extension in the Lemitar Mountains, central Rio Grande rift, *in* Keller, G.R., and Cather, S.M., eds., Basins of the Rio Grande Rift: Structure, Stratigraphy, and Tectonic Setting: Geological Society America, Special Paper 291, p. 157–170.

Celep, E., 2017, Lithofacies analysis of the Sierra Ladrones Formation, southern Albuquerque basin N.M.: Implications for the Cliff fault activity during the early Pleistocene [M.S. thesis]: Socorro, New Mexico Institute of Mining and Technology, 94 p.

Chamberlin, R.M., 1999, Preliminary geologic map of the Socorro 7.5-minute quadrangle: New Mexico Bureau of Geology and Mineral Resources, Open-File Report OF-GM 34, scale 1:24,000.

Chamberlin, R.M., and McIntosh, W.C., 2007, Chronology and structural control of Late Cenozoic volcanism in the Loma Creston quadrangle, southern Jemez volcanic field, New Mexico: New Mexico Geological Society, Guidebook 58, p. 248–261.

Chamberlin, R.M., Cather, S.M., Nyman, W.M., and McLemore, V.T., 2001, Preliminary geologic map of the Lemitar 7.5-minute quadrangle, Socorro County, New Mexico: New Mexico Bureau of Geology and Mineral Resources, Open-File Report OF-GM 38, scale 1:24,000.

Chamberlin, R.M., Love, D.W., Harrison, B.J., Lueth, V.W., Frey, B.A., Williams, S., and Connell, S.D., 2016, Sevilleta west: Pre-meeting road log from Sevilleta National Wildlife Refuge Visitor Center, to San Acacia, Cerritos de las Minas, West Mesa, and San Lorenzo Spring: New Mexico Geological Society, Guidebook 67, p. 37–61.

Chapin, C.E., 1971, The Rio Grande rift, Part 1: Modifications and additions: New Mexico Geological Society, Guidebook 22, p. 191–201.

Connell, S.D., 2008, Refinements to the stratigraphic nomenclature of the Santa Fe Group, northwestern Albuquerque Basin, New Mexico: New Mexico Geology, v. 30, p. 14–35.

Connell, S.D., and Lucas, S.G., 2001, Stratigraphic column of the Tio Lino section illustrating fluvial and piedmont facies of the Sierra Ladrones Fm, *in* Love, D.W., Connell, S.D., Lucas, S.G., Morgan, G.S., Derrick, N.N., Jackson-Paul, P.B., and Chamberlin, R., eds., Third-Day Road-log, April 29, 2001, Belen Sub-basin: Belen, Sevilleta National Wildlife Refuge, and Northern Socorro Basin: New Mexico Bureau of Mines and Mineral Resources, Open-file Report 454A, p. 38–41.

Connell S.D., and McCraw D.J., 2007, Geologic Map of the La Joya NW Quadrangle, Socorro County, N.M.: New Mexico Bureau of Geology and Mineral Resources, Open-file Digital Geologic Map OF-GM 140, scale 1:24,000.

Connell, S.D., Hawley, J.W., and Love, D.W., 2005, Late Cenozoic drainage development in the southeastern Basin and Range of New Mexico, southeasternmost Arizona and western Texas, *in* Lucas, S.G., Morgan, G.S., and Zeigler, K.E., eds., New Mexico's Ice Ages: New Mexico Museum Natural History and Science, Bulletin 28, p. 125–150.

Connell, S.D., Smith, G.A., Geissman, J.W., and McIntosh, W.C., 2013, Climatic controls on non-marine depositional sequences in the Albuquerque Basin, Rio Grande rift, north-central New Mexico, *in* Hudson, M.R., and Grauch, V.J.S., eds., New Perspectives on Rio Grande Rift Basins: From Tectonics to Groundwater: Geological Society of America, Special Paper 494, p. 383–425.

Davis, J.M., Lohmann, R.C., Phillips, F.M., Wilson, J.L., and Love, D.W., 1993, Architecture of the Sierra Ladrones Formation, central New Mexico: Depositional controls on the permeability correlation structure: Geological Society of America, Bulletin 105, p. 998–1007.

Fialko, Y., and Simons, M., 2001, Evidence for on-going inflation of the Socorro magma body, New Mexico, from interferometric synthetic aperture radar imaging: Geophysical Research Letters, v. 28, no. 18, p. 3549–3552.

Finnegan, N.J., and Pritchard, M.E., 2009, Magnitude and duration of surface uplift above the Socorro magma body: Geology, v. 37, p. 231–234.

Gillespie, C.L., Grauch, V.J.S., Oshetski, K., and Keller, G.R., 2000, Principal facts for gravity data collected in the southern Albuquerque Basin and a regional compilation, central New Mexico: United States Geological Survey, Open file Report 00-490.

Goff, F., and Shackley, M.S., 2022, Origin of archaeologically significant gravel and lag deposits on southwestern Horace Mesa, Mount Taylor Region, New Mexico [abstract]: New Mexico Geological Society, 2022 Annual Spring Meeting & Ft. Stanton Cave Conference, https://nmgs.nmt.edu/meeting/abstracts/view.cfm?aid=2789 (accessed 5/9/22).

Goff, F., Zimmerer, M., Krier, D., Goff, C.J., Shackley, M.S., Gehrz, J., and Niklasson, SA., 2021, Detailed investigations of Rendija Canyon Rhyodacite, a complicated volcanic complex in the Sierra de los Valles, Jemez Mountains volcanic field, New Mexico [abstract]: New Mexico Geological Society, 2021 Annual Spring Meeting, p. 23–24, https://nmgs.nmt.edu/meeting/abstracts/view.cfm?aid=2754 (accessed 5/9/22).

Grauch, V.J.S., and Connell, S.D., 2013, New perspectives on the geometry of the Albuquerque Basin, Rio Grande rift, New Mexico: Insights from geophysical models of rift-fill thickness: Geological Society of America, Special Paper 494, p. 427–462.

Hawley, J.W., compiler, 1978, Guidebook to Rio Grande rift in New Mexico and Colorado: New Mexico Bureau of Mines and Mineral Resources, Circular 163, 241 p.

Hawley, J.W., 2005, Five million years of landscape evolution in New Mexico: An overview based on two centuries of geomorphic conceptual-model development, *in* Lucas, S.G., Morgan, G.S., and Zeigler, KE., eds., New Mexico's Ice Ages: New Mexico Museum Natural History and Science, Bulletin 28, p. 9–94.

Hinojosa, J.R., 2021, Surface geologic mapping and subsurface characterization near the Loma Blanca fault, central New Mexico [Master's thesis]: Socorro, New Mexico Institute of Mining and Technology, 500 p.

Kelley, S.A., McIntosh, W.C., Goff, F., Kempter, K.A., Wolff, J., Esser, R., Braschayko, S., Love, D., and Gardner, J.N., 2013, Spatial and temporal trends in pre-caldera Jemez Mountains volcanic and fault activity: Geosphere, v. 9, no. 3, p. 1–33.

Kelley, V.C., 1977, Geology of the Albuquerque Basin: New Mexico Bureau of Mines and Mineral Resources, Memoir 33, 60 p.

Lipman, P.W., 2007, Incremental assembly and prolonged consolidation of Cordilleran magma chambers: Evidence from the Southern Rocky Mountain volcanic field: Geosphere, v. 3, no. 1, p. 42–70.

Love, D.W., and Rinehart A.J., 2016, Many paths to enlightenment in a feature-challenged landscape: Influence of Abo drainage on geomorphology across the southeastern Albuquerque Basin during Quaternary time: New Mexico Geological Society, Guidebook 67, p. 25–27.

Love, D.W., and Young, J.D., 1983, Progress report on the late Cenozoic geologic evolution of the lower Rio Puerco: New Mexico Geological Society, Guidebook 34, p. 277–284.

Love, D.W., McCraw, D.J., Chamberlin, R.M., Reiter, M., Connell, S.D., Cather, S.M., and Majkowski, L., 2009, Progress report on tracking Rio Grande terraces across the uplift of the Socorro magma body: New Mexico Geological Society, Guidebook 60, p. 415–424.

Love, D.W., Rinehart A., Chamberlin, R., Celep, E., and Koning, D., 2017, Implications of past extents of Rio Salado and Rio Puerco deposits in the southwestern corner of the Albuquerque Basin, New Mexico [abstract and presentation]: New Mexico Geological Society, 2017 Annual Spring Meeting, p. 46, https://nmgs.nmt.edu/meeting/abstracts/view.cfm?aid=535 (accessed 5/9/22)

Love, D.W., Celep, E., McCraw, D.J., and Koning, D., this volume, Summary of the stratigraphy of both foot- and hanging-wall exposures of the Cliff fault, southern embayment of the Albuquerque Basin, Socorro County, New Mexico: New Mexico Geological Society, Guidebook 72.

Lozinsky, R.P., Hawley, J.W., and Love, D.W., 1991, Geologic overview and Pliocene-Quaternary history of the Albuquerque Basin, central New Mexico, *in* Julian, B., and Zidek, J., eds., Field guide to geologic excursions in New Mexico and adjacent areas of Texas and Colorado: New Mexico Bureau of Mines and Mineral Resources, Bulletin 137, p. 157–162.

Machette, M.N., 1978, Geologic map of the San Acacia quadrangle, Socorro County, New Mexico: U.S. Geological Survey, Geologic Quadrangle Map GQ-1415, scale 1:24,000.

Machette, M.N., and McGimsey, R.G., 1983, Quaternary and Pliocene faults in the Socorro and western part of the Fort Sumner 1° x 2° quadrangle, New Mexico: U.S. Geological Survey, Miscellaneous Field Studies Map MF-1465-A, 1:250,000 scale.

McCraw, D.J., 2016, A geologic summary of the Llano de Albuquerque: A diachronous ~1.8-1.65 (?) Ma geomorphic surface complex marking the cessation of Santa Fe Group deposition in the western Albuquerque Basin: New Mexico Geological Society, Guidebook 67, p. 83–85.

Morgan, G.S., Sealey, P.S., and Lucas, S.G., 2008, Pliocene (Blancan) vertebrates from Arroyo de la Parida, Palomas Formation, Socorro County, central New Mexico: New Mexico Museum of Natural History and Science, Bulletin 44, p. 189–206.

Morgan, G.S., Lucas, S.G., and Love, D.W., 2009, Cenozoic vertebrate faunas from Socorro County, central New Mexico: New Mexico Geological Society, Guidebook 60, p. 321–336.

Phillips, F.M., and Sion, B.D., this volume, Geomorphic surfaces of the Rio Grande Valley in the vicinity of Socorro, New Mexico: New Mexico Geological Society, Guidebook 72.

Reiter, M., Chamberlin, R.M, and Love, D.W., 2010, New data reflect on the thermal antiquity of the Socorro magma body locale, Rio Grande rift, New Mexico: Lithosphere, v. 2, no. 6, p. 447–453.

Repasch, M., Karlstrom, K.E., Heizler, M.T., and Pecha, M., 2017, Birth and evolution of the Rio Grande fluvial system in the past 8 Ma: Progressive downward integration and the influence of tectonics, volcanism, and climate: Earth Science Reviews, v. 168, p. 113–164.

Sion, B.D., Phillips, F.M., Axen, G.J., Harrison, J.B.J., Love, D.W., and Zimmerer, M.J., 2020, Chronology of terraces in the Rio Grande rift, Socorro basin, New Mexico: Implications for terrace formation: Geosphere, v. 16, 22 p.

Steiger, R.H., and Jäger, E., 1977, Subcommission on geochronology: Convention on the use of decay constants in geo-and cosmochronology: Earth and Planetary Science Letters, v. 36, no. 3, p. 359–362.

Taylor, J.R., 1982, An Introduction to Error Analysis: The Study of Uncertainties in Physical Measurements: Mill Valley, CA, University Science Books, 270 p.

U.S. Geological Survey, 2022, Quaternary fault and fold database of the United States, https://earthquake.usgs.gov/cfusion/qfault/query_results_AB_advanced.cfm (accessed 4/29/22).

Williams R.T., Goodwin, L.B., Warren, D.S., and Mozley, P.S., 2017, Reading a 400,000-year record of earthquake frequency for an intraplate fault: Proceedings of the National Academy of Sciences, v. 114, no. 19, p. 4893–4898.

Williams, R.T., Mozley, P.S., Sharp, W.D., and Goodwin, L.B., 2019, U□Th dating of syntectonic calcite veins reveals the dynamic nature of fracture cementation and healing in faults: American Geophysical Union, Geophysical Research Letters, v. 46. p. 12900–12908.

Woodward, L.A., Callender, J.F., Seager, W.R., Chapin, C.E., Gries, J.C., Shaffer, W.L., and Zilinski, R.E., 1978, Tectonic map of the Rio Grande rift region in New Mexico, Chihuahua, and Texas, *in* Hawley, J.W., compiler, Guidebook to Rio Grande rift in New Mexico and Colorado: New Mexico Bureau of Mines and Mineral Resources, Circular 163, sheet 2, in pocket, 1:1,000,000 scale.

Young, J.D., and Love, D.W., 2016, Grants obsidian in the Ceja Formation beneath the Llano de Albuquerque south of Belen: New Mexico Geological Society, Guidebook 67, p. 22–24.

Zimmerer, M.J., and McIntosh, W.C., 2011, $^{40}Ar/^{39}Ar$ dating, sanidine chemistry, and potential sources of the Las Tablas Tuff, northern New Mexico: New Mexico Geological Society, Guidebook 62, p. 215–221.

Appendices can be found at
https://nmgs.nmt.edu/repository/index.cfml?rid=2022003

View to northeast of the San Acacia diversion dam, where water is diverted into a major canal that delivers waters to farms in the Socorro area. In the left-background is “Indian Mesa,” which is capped by the 4.9 Ma trachyandesite of San Acacia (age from Chamberlin et al., 2001). Below this volcanic flow lies reddish, fine-grained sandstones (right) and whitish, coarser sand and gravelly sands (left) interpreted as distal piedmont-alluvial flat and axial-fluvial facies of the Sierra Ladrones Formation, respectively. These two sedimentary facies are separated by a west-down fault that projects to the west-down Cliff fault (Machette, 1978). Photo by Dave Love.